8-13-1991

Active Control of Convection

Jonathan Singer
University of Pennsylvania

Haim H. Bau
University of Pennsylvania, bau@seas.upenn.edu

Active Control of Convection

Abstract
It is demonstrated theoretically that active (feedback) control can be used to alter the characteristics of thermal convection in a toroidal, vertical loop heated from below and cooled from above. As the temperature difference between the heated and cooled sections of the loop increases,t he flow in the uncontrolled loop changes from no motion to steady; time independent motion to temporally oscillatory, chaotic motion. With the use of a feedback controller effecting small perturbations in the boundary conditions, one can maintain the no-motion state at significantly higher temperature differences than the critical one corresponding to the onset of convection in the uncontrolled system. Alternatively, one can maintain steady, time-independent flow under conditions in which the flow would otherwise be chaotic. That is, the controller can be used to suppress chaos. Likewise, it is possible to stabilize periodic nonstable orbits that exist in the chaotic regime of the uncontrolled system. Finally, the controller also can be used to induce chaos in otherwise laminar (fully predictable), nonchaotic flow.

Disciplines
Engineering | Mechanical Engineering

Comments
Suggested Citation:
Singer, Johnathan and Haim H. Bau. (1991). *Active control of convection.* Journal of Applied Physics. Vol. 3(12).

Active control of convection

Jonathan Singer and Haim H. Bau[a)]
Department of Mechanical Engineering and Applied Mechanics, University of Pennsylvania, Philadelphia, Pennsylvania 19104-6315

(Received 16 April 1991; accepted 13 August 1991)

It is demonstrated theoretically that active (feedback) control can be used to alter the characteristics of thermal convection in a toroidal, vertical loop heated from below and cooled from above. As the temperature difference between the heated and cooled sections of the loop increases, the flow in the uncontrolled loop changes from no motion to steady, time-independent motion to temporally oscillatory, chaotic motion. With the use of a feedback controller effecting small perturbations in the boundary conditions, one can maintain the no-motion state at significantly higher temperature differences than the critical one corresponding to the onset of convection in the uncontrolled system. Alternatively, one can maintain steady, time-independent flow under conditions in which the flow would otherwise be chaotic. That is, the controller can be used to suppress chaos. Likewise, it is possible to stabilize periodic nonstable orbits that exist in the chaotic regime of the uncontrolled system. Finally, the controller also can be used to induce chaos in otherwise laminar (fully predictable), nonchaotic flow.

I. INTRODUCTION

In recent years, active control has been successfully used in many engineering applications such as noise reduction and vibration suppression in automobiles and airplanes. The area of active control of convective processes is no less important from a technological point of view. In some processes, it may be desirable to operate at Rayleigh numbers higher than the one at which convection occurs and yet have no convection. In other processes, it may be desirable to suppress (*laminarize*[1]) chaotic or turbulent motions and maintain a steady, time-independent flow in order to minimize flow unpredictability, remove temperature oscillations which may exceed safe operational conditions, and/or reduce drag. In still other processes, it may be advantageous to induce chaos under conditions at which it would not normally occur, so as to enhance mixing, heat transport, or chemical reactions. Despite the foregoing, the idea of using active (feedback) control to modify convective motion by suppressing or enhancing naturally occurring disturbances in the flow seems to have attracted little attention.

In recent work,[2] we have demonstrated experimentally that one can use active (feedback) control to suppress the naturally occurring chaotic motion in a thermal convection loop. The experimental apparatus used was similar to the one employed by Creveling *et al.*[3] and Gorman *et al.*[4] The apparatus consisted of a tube bent into a torus and positioned in the vertical plane. The lower and upper halves of the loop were heated and cooled, respectively, with the thermal boundary conditions being nominally time-independent and symmetric with respect to the loop's axis that is parallel to the gravity vector. For the uncontrolled loop, we observed that for relatively low heating rates the flow was time independent. For heating rates above some critical value, the flow became time dependent with oscillations in the flow rate and occasional reversals in the flow direction. We showed that with the use of a controller, it is possible to maintain time-independent motion in conditions under which the flow in the uncontrolled system is chaotic. The control strategy consisted of sensing the temperature at a number of points inside the fluid and modifying slightly the wall temperature in proportion to the deviations of the measured quantities from prescribed values.

In this paper, we develop a theory that explains how a feedback controller can modify the flow regimes in the loop. In the first part of the paper, we demonstrate that through the use of the controller one can stabilize the no-motion state. That is, no motion can be sustained well beyond the critical Rayleigh number associated with the onset of convection in the uncontrolled system. In the second part of the paper, we demonstrate how time-independent flow can be maintained in conditions under which flow in the uncontrolled system is chaotic. We also show that, if desired, the controller can be used to destabilize the flow. In the last part of the paper, we follow up on ideas articulated by Ott *et al.*[5] and demonstrate that with an adequate control strategy one can obtain still other flow structures in the loop. Unfortunately, since our experimental apparatus is not sufficiently refined, many of the ideas presented here still await experimental confirmation. Nevertheless, the success we reported in Singer *et al.*[2] suggests that at least some of these ideas can actually be implemented.

Our main reason for choosing the thermal convection loop for study is that the convective motion in the loop can be described by a relatively simple mathematical model which still maintains much of the physics of the process. We hope that the insights we gain from this study can be applied to more complicated processes such as Bénard convection. In any case, the system chosen for study is relevant to many technological processes since thermal convection loops provide a means for circulating fluid without the use of pumps. Such loops are of interest for solar heaters, emergency reac-

a) All correspondence should be directed to this author.

 0899-8213/91/122859-07$02.00

tor-core cooling, and process industries. They also are of interest for understanding warm springs, seawater circulation in the oceanic crust, and formation of ore deposits. For a general review of applications and analyses of these loops, see the paper by Metrol and Greif[6] and the literature cited therein.

II. MATHEMATICAL MODEL

Consider a thermal convection loop constructed from a pipe bent into a torus and standing in the vertical plane as depicted in Fig. 1. The diameter of the pipe is d, the diameter of the torus is D, and θ is the angular location of a point on the torus. The prescribed wall temperature of the pipe $T_w(\theta,t)$ may vary both with the angular location θ and time t. Variations in the wall temperature may cause a temperature gradient to form inside the fluid. This, in turn, may induce fluid motion in the loop under appropriate conditions.

We analyze the motion in the loop within the framework of Boussinesq's approximation using a one-dimensional model consisting of mass, momentum, and energy balances:[7]

$$u = u(t), \tag{1}$$

$$\dot{u} = \frac{1}{\pi}\,\mathrm{Ra}\,P \oint T\cos(\theta)\,d\theta - Pu, \tag{2}$$

and

$$\dot{T} = -u\frac{\partial T}{\partial \theta} + B\frac{\partial^2 T}{\partial \theta^2} + [T_w(\theta,t) - T]. \tag{3}$$

The fluid is assumed to be incompressible and Newtonian. In the above, all quantities are nondimensional. Here, $\mathrm{Ra} = g\beta\Delta T\tau^2/DP$ is the loop's Rayleigh number; β is the thermal expansion coefficient; g is the gravitational acceleration; and ΔT is the averaged wall temperature difference between the loop's bottom and top. The time scale is $\tau = \rho_0 C_p d/(4h)$, where ρ_0 is the fluid's average density, C_p is the thermal capacity, and h (which we assume to be constant) is the heat transfer coefficient between the fluid and the pipe's wall. Here $P = 32\nu\tau/d^2 = 8\ \mathrm{Pr}/\mathrm{Nu}$ is the loop's Prandtl number, where ν is the kinematic viscosity; $\mathrm{Pr} = \nu/\alpha$ and $\mathrm{Nu} = hd/k$ are the conventional Prandtl and Nusselt numbers, respectively; α and k are the fluid's thermal diffusivity and conductivity; and $B = (d/D)^2/\mathrm{Nu}$ is the Biot number. The length scale is the torus' radius $D/2$.

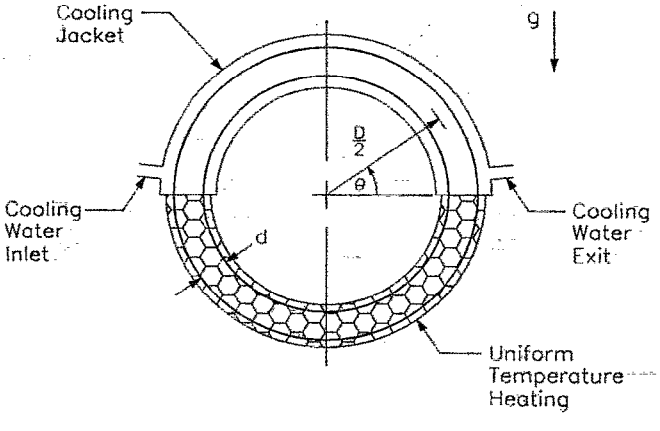

FIG. 1. Schematic description of the experimental apparatus.

In addition to the aforementioned Boussinesq approximation, the mathematical model presented here assumes implicitly that the friction and heat transfer laws are similar to those of laminar, fully developed, Poiseuille pipe flow. One would expect and we did, in fact, observe in the experiments the development of secondary circulation which may significantly modify both the friction and heat transfer laws (but has the positive effect of improving temperature uniformity at each cross section of the loop). Unfortunately, more realistic friction and heat transfer laws are not *a priori* known. To obtain these correlations, one may need to solve a spatially three-dimensional model or conduct experiments. We justify the use of the simpler correlations above on the grounds that the model still provides a qualitatively correct picture as has been confirmed by our own experiments[8] and those of others[9] as well as by theoretical studies by Hart[10] and Yorke *et al.*,[11] in which more complicated heat transfer and friction factor correlations were used.

Next, we expand the wall (T_w) and fluid (T) temperatures in Fourier series in terms of the angle θ with the sine and cosine terms corresponding, respectively, to symmetric and asymmetric temperature distributions with respect to the loop's axis that is parallel to the gravity vector:

$$T_w(\theta,t) = W_0(t) + \sum_{n=1}^{\infty} W_n(t)\sin(n\theta) + V_n(t)\cos(n\theta), \tag{4}$$

and

$$T(\theta,t) = C_0(t) + \sum_{n=1}^{\infty} S_n(t)\sin(n\theta) + C_n(t)\cos(n\theta). \tag{5}$$

Upon substituting the series (4) and (5) into the governing equations (1)–(3) and requiring that these equations are satisfied in the sense of weighted residuals, we obtain an infinite set of ordinary differential equations. Three equations which are similar to the celebrated Lorenz equations[12] decouple from the rest of the set (with exact closure) and can be solved independently of the other equations without need of truncation.[13] The full dynamics of the problem can be described by these three equations:

$$\dot{u}/P = c - u, \tag{6}$$

$$\dot{c} = -us - c + \mathrm{Ra}\,V_1, \tag{7}$$

$$\dot{s} = uc - s + \mathrm{Ra}\,W_1. \tag{8}$$

In the above, we removed the dependence on the Biot number B via the simple, algebraic transformation $\{u, c, s, \mathrm{Ra}, P, t\} \leftarrow 1/(1+B)\ \{u, \mathrm{Ra}\,C_1, \mathrm{Ra}\,S_1, \mathrm{Ra}/(1+B), P, t(1+B)^2\}$. Roughly speaking, the quantities c and s are proportional, respectively, to the temperature differences between positions 3 and 9 and 6 and 12 o'clock around the loop.

III. THE UNCONTROLLED FLOW—A SUMMARY

In this section, we review briefly the flow regimes observed in a loop in which the heating and cooling boundary

conditions are fixed in time and symmetric with respect to the loop's axis that is parallel to the gravity vector. The required symmetry is obtained in Eqs. (6)–(8) by setting $V_1 = 0$. Also, without loss of generality, we set $W_1 = -1$. Equations (6)–(8) with the aforementioned modifications are the celebrated Lorenz equations and have been investigated exhaustively in the literature.[14] The equations possess a number of nontransient solutions:

(A) no-motion state ($u = c = 0, s = -\mathrm{Ra}$);

(B) time-independent motion either in the clockwise (denoted B_-) or counterclockwise (denoted B_+) direction ($u = c = \pm\sqrt{\mathrm{Ra} - 1}, s = -1$);

(C) chaotic motion;

(D) periodic motions of various periodicities.

These various solutions and their stability characteristics are shown in the bifurcation diagram depicted in Fig. 2 for a loop Prandtl number $P = 4$ which we estimate to approximate the loop Prandtl number of our experimental apparatus. In the figure, we denote stable and nonstable solutions by solid and dashed lines, respectively. Briefly, if one were to follow the chain of events as the Rayleigh number (Ra) increases, one would observe no net motion in the loop for $\mathrm{Ra} < 1$. At $\mathrm{Ra} = 1$, the no-motion solution loses its stability through a supercritical pitchfork bifurcation and is replaced by time-independent motion. Depending on random disturbances, this motion may be either in the clockwise (B_-) or counterclockwise (B_+) direction. The motion solution is stable for $1 < \mathrm{Ra} < \mathrm{Ra}_H(P) = P(P+4)/(P-2)$, where $\mathrm{Ra}_H(4) = 16$. At this point, the steady solution loses stability through a subcritical Hopf bifurcation. The resulting limit cycle is nonstable and its period increases to infinity as the Rayleigh number decreases to $\mathrm{Ra}_{\mathrm{hom}}(P)$. At $\mathrm{Ra}_{\mathrm{hom}}(4) \sim 7.378$, the periodic orbit (known as an homoclinic orbit) passes through the no-motion state (A). At the homoclinic point, there is a bifurcation (the homoclinic explosion) that results in an assortment of nonstable periodic and nonperiodic orbits known collectively as the nonwandering set. As the Rayleigh number is further increased beyond $\mathrm{Ra}_A(P) < \mathrm{Ra}_H(P)$, where $\mathrm{Ra}_A(4) \sim 15.984$, the nonwandering set becomes a strange (the Lorenz) attractor. The chaotic regime exists for $\mathrm{Ra} > \mathrm{Ra}_A$ with occasional windows of periodic behavior. In the chaotic regime, the motion in the loop consists of irregular oscillations with occasional reversals in the direction of the flow as shown, for example, in Fig. 3 for $P = 4$ and $\mathrm{Ra} = 3\mathrm{Ra}_H(4)$. In Figs. 3(a) and 3(b), we depict, respectively, the temperature differences between positions 3 and 9 o'clock (c) and positions 12 and 6 o'clock (s) as functions of time. The positive and negative values in Fig. 3(a) correspond to flow in the counterclockwise and clockwise directions, respectively. Qualitatively similar behavior was observed in our experiments.

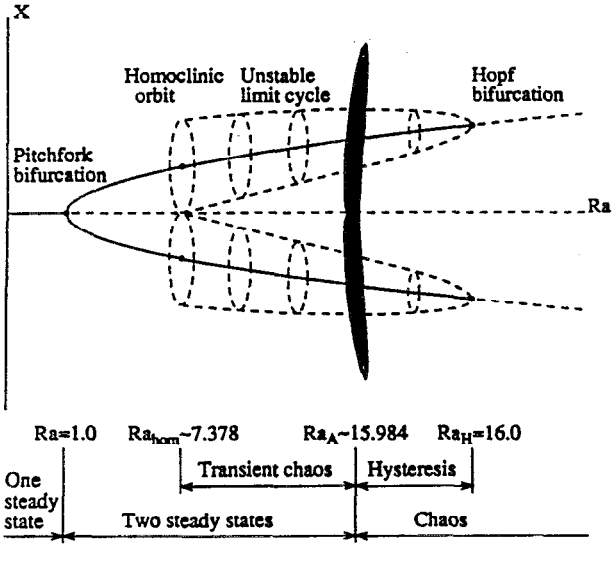

FIG. 2. An unscaled bifurcation diagram depicting various possible solutions as the Rayleigh number is increased ($P = 4$). Stable and nonstable solutions are denoted by solid and dashed lines, respectively. The dark region represents the appearance of the strange attractor which exists for $\mathrm{Ra} > \mathrm{Ra}_A$.

IV. STABILIZATION OF THE NO-MOTION STATE

In this section, we examine the feasibility of using active control to affect the stability of the no-motion state. We assume that one can measure in an experiment the temperature difference (c) between positions 3 and 9 o'clock around the loop and/or the fluid velocity (u). In the no-motion state, we wish to maintain the above two quantities at a zero value (i.e., $u = c = 0$). That is, we shall attempt to suppress any

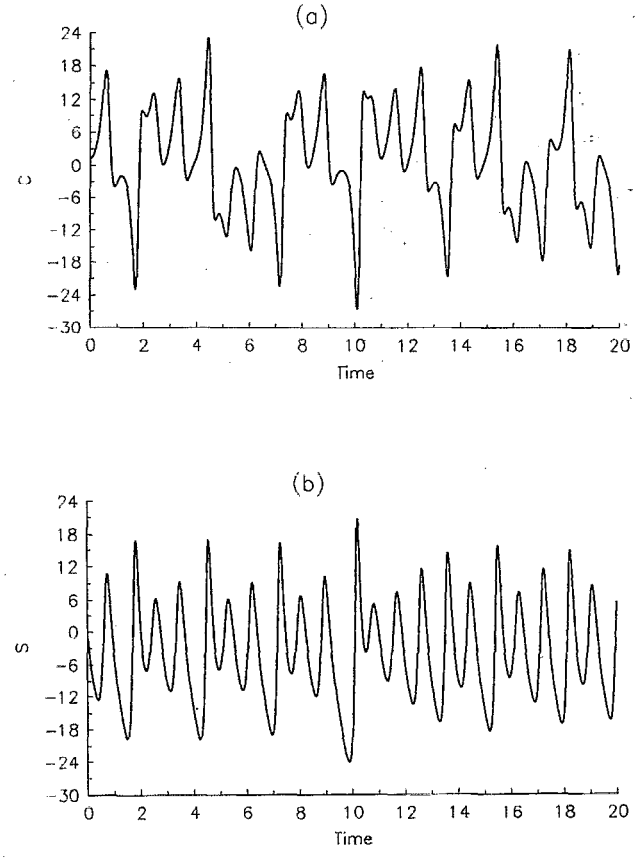

FIG. 3. The temperature difference between positions 3 and 9 o'clock (a) and 6 and 12 o'clock (b) is depicted as a function of time for $\mathrm{Ra} \sim 3\mathrm{Ra}_H = 48$.

disturbances which lead to deviations from these desired values. This can be done, for example, by applying asymmetric perturbations to the wall temperature in proportion to the deviations of u and c from their desired magnitudes. To this end, we set the controller to provide $V_1 = (K_u u + K_c c)/\mathrm{Ra}$, where K_u and K_c are the controller's gains. It turns out that the no-motion state cannot be stabilized by applying similar disturbances symmetrically with respect to the loop's axis that is parallel to the gravity vector. The equations for the controlled system are

$$\dot{u}/P = c - u, \tag{9}$$

$$\dot{c} = -uz + \mathrm{Ra}\,u - c + K_u u + K_c c, \tag{10}$$

$$\dot{z} = uc - z, \tag{11}$$

where $z = s + \mathrm{Ra}$, and, without loss of generality, we set $W_1 = -1$ in Eq. (8). The controlled system (9)–(11) admits the no-motion solution (A) $u = c = z = 0$ which is identical to the no-motion solution of the uncontrolled system and the two time-independent motion solutions $(u = c = \pm\sqrt{\mathrm{Ra} + K_u + K_c - 1}, z = \mathrm{Ra} + K_u + K_c - 1)$ corresponding to counterclockwise and clockwise circulation in the loop.

Stability analysis reveals that the no-motion state is linearly stable for $\mathrm{Ra} < \mathrm{Ra}_L = 1 - K_u - K_c$ and globally stable for $\mathrm{Ra} < \mathrm{Ra}_G = \mathrm{Min}(1 - K_u - 2K_c, 1 - K_u)$. That is, negative gains stabilize the no-motion state while positive gains destabilize it. For illustration purposes, we show in Fig. 4 (where $\mathrm{Ra} = 5$) the velocity (u) in the loop as a function of time for the controlled system ($K_u = K_c = -2.5$, heavy line) and the uncontrolled system ($K_u = K_c = 0$, dotted line). In the controlled system, the velocity decays to a zero value for all initial conditions. Recall that for the uncontrolled system, the no-motion state can be maintained only for $\mathrm{Ra} < 1$.

To illustrate the controller's effect from a physical point of view, let us briefly recall why the no-motion state becomes unstable in the uncontrolled system. In the no-motion state, the fluid's temperature is at equilibrium with the wall temperature. In a loop heated from below and cooled from above $(\mathrm{Ra} > 0)$, we have cold (heavier) fluid overlaying hotter (lighter) fluid. This arrangement is gravitationally unstable.

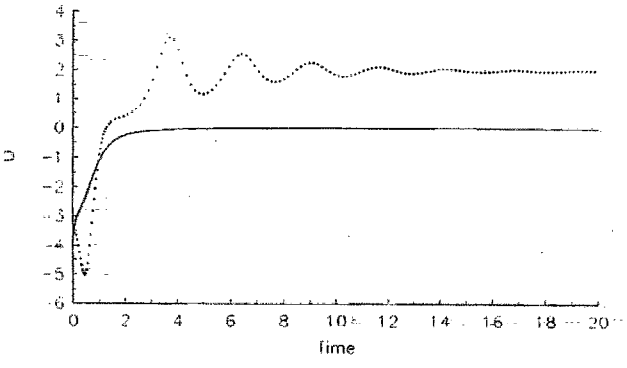

FIG. 4. Stabilization of the no-motion state. The velocity u in the controlled system (solid line) decays to zero as a function of time for $\mathrm{Ra} = 5$ and $K_u = K_c = -2.5$. In contrast, the velocity in the uncontrolled system (dashed line) attains the value of 2 after initial transients die out.

Small, asymmetric thermal disturbances naturally occurring in the fluid will tend to give rise to a buoyancy force and to fluid motion either in the clockwise or the counterclockwise direction. Ironically, in the absence of such fluid motion, these disturbances eventually would disappear due to dissipation and heat exchange with the pipe's walls. However, with the onset of fluid motion, the temperature difference between the ascending and descending fluid tends to increase, thus providing a further increase in the buoyancy force and a mechanism for the disturbance to manifest itself. In the uncontrolled system, these two effects are of equal importance at the critical Rayleigh number for the onset of convection ($\mathrm{Ra} = 1$). In the controlled system, when a disturbance occurs, the feedback control adjusts the wall temperature so as to enhance the disturbance dissipation process, thus shifting the balance between disturbance dissipation and amplification to higher Rayleigh numbers and, in effect, stabilizing the no-motion state.

It should be noted that the control strategy we have described above is not the only possible one, nor is it necessarily the best. A different control strategy might include, for example, the application of angular acceleration to the loop.

V. CHAOS SUPPRESSION OR ENHANCEMENT

In the uncontrolled, symmetrically heated system $(V_1 = 0)$, the time-independent motion solution loses its stability at Ra_H through a subcritical Hopf bifurcation. For $\mathrm{Ra} > \mathrm{Ra}_H$, the time-independent convection is replaced by oscillatory, chaotic motion. In this section, we examine the possibility of using active control to stabilize or destabilize the steady-state solution (B_+). We begin by trying to obtain steady, nonoscillatory flow under conditions in which the uncontrolled flow is nominally chaotic $(\mathrm{Ra} > \mathrm{Ra}_H)$. Later, we examine the possibility of obtaining chaotic motion for $\mathrm{Ra} < \mathrm{Ra}_H$.

In the experimental apparatus, we measure the temperature difference between locations 6 and 12 o'clock (s) around the loop and we adjust the loop's wall temperature by varying the power input to our heater. Thus, we use this temperature difference as the controlling signal and the power input as the controlled signal.

For the time-independent solution at Ra, $s(t) = \bar{s} = -1$. For $\mathrm{Ra} > \mathrm{Ra}_H$, this solution is nominally nonstable and $s(t)$ varies as a function of time in a rather complicated way [see Fig. 3(b) for an example]. We wish to modify the wall temperature so as to retain $s(t) = \bar{s}$. To this end, we use proportional control. The wall temperature is changed in proportion to the deviation of $s(t)$ from the desired value $\bar{s}$. We set $W_1 = -[1 + (K_s/\mathrm{Ra})(s + 1)]$ and the equations of motion assume the form

$$\dot{u}/P = c - u, \tag{12}$$

$$\dot{c} = -us - c, \tag{13}$$

$$\dot{s} = uc - s - \mathrm{Ra} - K_s(s + 1), \tag{14}$$

where K_s is the controller's gain. Note that Eq. (12)–(14) maintain the same invariance as the Lorenz equations. Thus we may expect that the controller will have a similar effect on both the counterclockwise motion (B_+) and the clock-

wise motion (B_-). A somewhat similar control strategy was employed by Vincent and Yu[15] to stabilize the B_+ orbit of the Lorenz equations.

The time-independent solutions of the controlled system (12) and (13) include the no-motion solution, $[u=c=0, s=-(\mathrm{Ra}+K_s)/(1+K_s)]$, and the two motion solutions, ($B_\pm: u=c=\sqrt{\mathrm{Ra}-1}, s=-1$). The latter are identical to the motion solutions of the uncontrolled system. Note that the effective Rayleigh number for the no-motion solution $\mathrm{Ra}_{\mathrm{eff}}=(\mathrm{Ra}+K_s)/(1+K_s)$ and that this solution is stable for $\mathrm{Ra}_{\mathrm{eff}}<1$. Thus the stability characteristics of the no-motion solution are not altered by the action of the controller.

Next, we establish the stability characteristics of the time-independent motion solutions. To this end, we carry out linear stability analysis around the solutions $B_\pm$. The characteristic equation for the growth rate of small disturbances (σ) is

$$\sigma^3+\sigma^2(2+K_s+P)+\sigma[K_s(1+P)+P+\mathrm{Ra}] +2P(\mathrm{Ra}-1)=0. \tag{15}$$

One of the roots of (15) is always real and negative. The other two roots are a complex conjugate pair with their real part being negative for $\mathrm{Ra}<\mathrm{Ra}^{\mathrm{H}}(P,K_s)$, where

$$\mathrm{Ra}^{\mathrm{H}}(P,K_s)=\frac{K_s(2+K_s+P)(1+P)P(4+K_s+P)}{P-2-K_s} \tag{16}$$

and $\partial\sigma/\partial\,\mathrm{Ra}>0$. Thus the loss of stability occurs through a Hopf bifurcation. We did not calculate directly the resulting limit cycle; but since the bifurcation is subcritical[16] for $K_s=0$, we also expect it to be subcritical and therefore nonstable for small K_s values.

The marginal stability limits for the time-independent motion solution are depicted in Fig. 5. Clearly, positive values of K_s stabilize the motion solution and delay the Hopf bifurcation while negative values of K_s destabilize the same solution. The effect of K_s on the root locus of Eq. (15) is depicted in Figs. 6(a) ($K_s>0$) and 6(b) ($K_s<0$) for $\mathrm{Ra}=50$ and 5, respectively. For $\mathrm{Ra}=50$ and $K_s=0$, the complex pair has a positive real part. As K_s increases, the real part of σ decreases and crosses the imaginary axis at

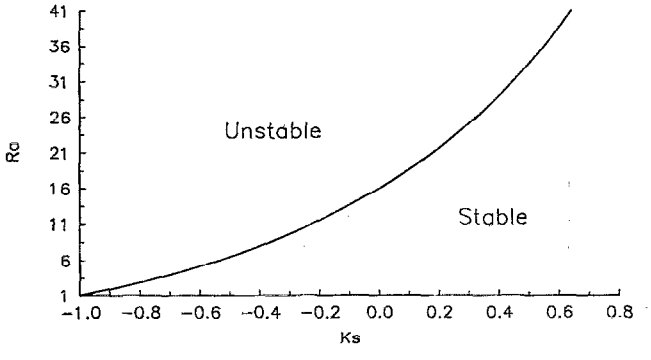

FIG. 5. Stability characteristics of the time-independent, motion solution under proportional control. The critical Rayleigh number is depicted as a function of the controller's gain (K_s).

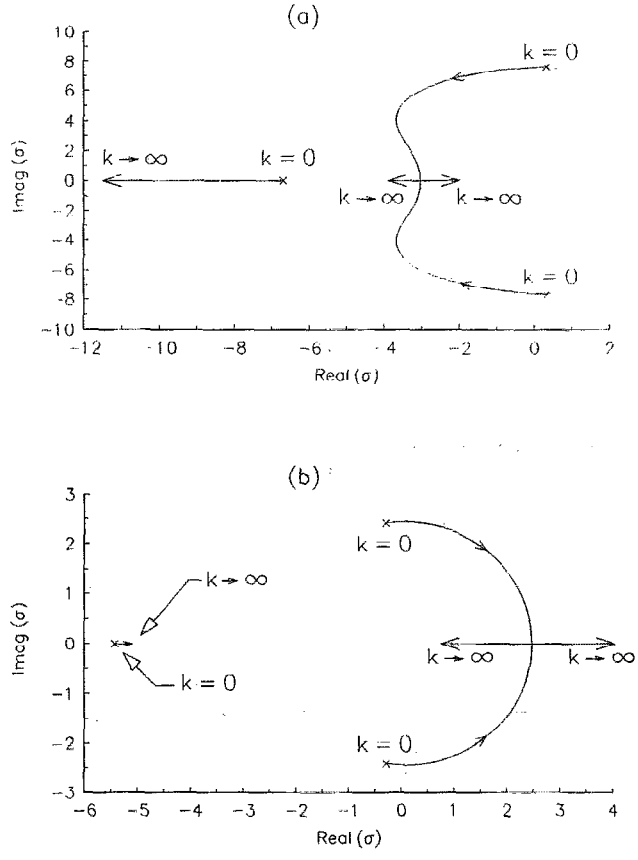

FIG. 6. The eigenvalues of Eq. (15) are depicted in the complex plane as functions of the controller's gain for (a) $K_s>0$, $\mathrm{Ra}=50$ and (b) $K_s<0, 5$, respectively; $P=4$.

$K_s\sim 0.774$. For higher values of the gain K_s, the time-independent motion solution becomes stable. As the imaginary part of σ decreases to zero, the controller will tend to damp any oscillatory motion.

The effect of the controller on the system is illustrated in Fig. 7, where we depict u as a function of time for both the uncontrolled ($K_s=0$, dashed line) and controlled ($K_s=2$, solid line) systems and for $\mathrm{Ra}=50$. The impact of the controller is fairly dramatic. While the uncontrolled system exhibits chaotic behavior, the controlled system behaves in a time-independent fashion.

The bifurcation diagram for the controlled system ($K_s>0$) is similar to the one depicted in Fig. 2 for the uncontrolled system. As K_s increases, the Hopf bifurcation point Ra_{H} moves to the right and so does the point Ra_A at which the nonwandering set becomes a strange attractor. Numerical experiments reveal, however, that Ra_{H} moves to the right faster than Ra_A. Thus, there will be an interval in parameter space (wider than in the uncontrolled system) in which both the chaotic attractor and the time-independent motion solutions coexist. For example, for $\mathrm{Ra}=26$, $\mathrm{Ra}^{\mathrm{H}}=33.5$, and $K_s=0.5$, depending on initial conditions, we observed either time-independent or chaotic motion. In such an interval, the time-independent solution has a basin of attraction that extends up to the nonstable periodic orbit generated at the Hopf bifurcation point. In practical terms,

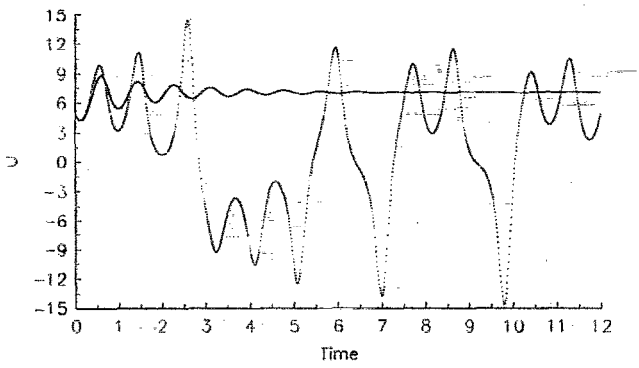

FIG. 7. The temperature difference between position 3 and 9 o'clock is depicted for $\mathrm{Ra} = 50$ and $P = 4$ as a function of time for the controlled ($K_s = 2$, solid line) and the uncontrolled ($K_s = 0$, dashed line) systems.

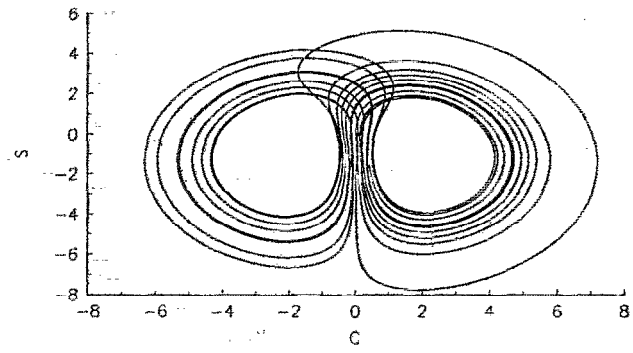

FIG. 8. Destabilization of stable solutions. The "*cs*" projection of the attractor's phase portrait for $\mathrm{Ra} = 5$, $K_s = -0.7$, and $P = 4$.

this implies that the controller can stabilize the time-independent solution only if applied when the system's trajectory in phase space is inside the aforementioned basin of attraction. Alternatively, if conditions permit, one may apply the controller at $\mathrm{Ra} < \mathrm{Ra}_H$ and keep it active while increasing the Rayleigh number, thus assuring that system trajectories are always within the basin of attraction of the solution we wish to control.

To illustrate how the controller operates, we briefly describe the mechanism responsible for the chaotic, oscillatory behavior of the flow in the loop.[17] To this end, imagine that a small disturbance causes the flow to slow down below the steady-state flow rate. As a result, the fluid spends more time in the heater/cooler section, gains/loses more/less heat than usual and emerges from the heater/cooler with a temperature higher/lower than usual. This, in turn, causes an increase in the buoyancy force with a corresponding increase in the fluid's velocity. Once the fluid velocity increases, the reverse of this process occurs with a subsequent reduction in the fluid velocity. Under appropriate conditions, these oscillations amplify and eventually lead to the chaotic behavior depicted in Fig. 3. With the controller, this transition to chaos may be avoided. The controller detects the appearance of disturbances by monitoring deviations in the temperature difference $s(t) - \bar{s}$. Once a deviation is detected, the controller takes action to counteract the effect of this deviation.

Next, we examine the possibility of destabilizing the flow or, in other words, inducing chaos under conditions in which it would not normally occur. Our linear stability analysis suggests that negative values of K_s destabilize the time-independent motion solution. We were able to obtain chaotic flows for nominal Rayleigh numbers as low as $\mathrm{Ra} = 5$ with $K = -0.7$. See, for example, Fig. 8, where we depict the "*cs*" projection of phase space trajectories for $P = 4$. Recall that the transition to chaos in the uncontrolled system does not occur until $\mathrm{Ra} = 16$.

VI. STABILIZATION OF OTHER MOTION SOLUTIONS

The chaotic attractor includes an assortment of periodic and quasiperiodic orbits of various periodicities. Here we focus only on the periodic orbits. We label the periodic orbits according to the number of times their trajectories in phase space circle around the fixed points B_+ and B_-. For example, the orbit of the periodic solution $B_+ B_-$ circles once around B_+ and once around B_-. The periodic solution $B_+ B_+ B_-$ consists of two cycles around B_+ and one around B_-. The various periodic orbits can be obtained by examining Poincaré sections of the phase portrait generated either from trajectories obtained numerically or reconstructed from an experimental time series using the time delay technique.[18] Ott *et al.*[5] recently proposed a technique to stabilize nonstable periodic orbits residing within the chaotic attractor. Inspired by their work, we apply a somewhat different technique below.

We use a proportional controller to stabilize a $B_+ B_-$ orbit. Other orbits can be stabilized in a similar fashion. We begin by identifying $s(t) = s_T(t)$ with $s_T(t + T) = s_T(t)$ values which correspond to the nonstable $B_+ B_-$ orbit we wish to stabilize. Next, we change the wall temperature $W_1 = -1 + K(s - s_T)$ in proportion to the deviation of s from its desired value (s_T). As $s_T(t)$ may be known only in a numerical form, we store the values of s_T in a table. The results of this control strategy are depicted in Fig. 9 for $\mathrm{Ra} = 50$, $P = 4$, and $K = 5$, where we show the projection of the periodic orbit on the "*cs*" plane of phase space. Light and heavy lines in Fig. 9 denote the transient and stabilized periodic orbits, respectively. We note in passing that it may suffice to activate the controller just once within each period as has been successfully done by Ott *et al.*[5] in numerical

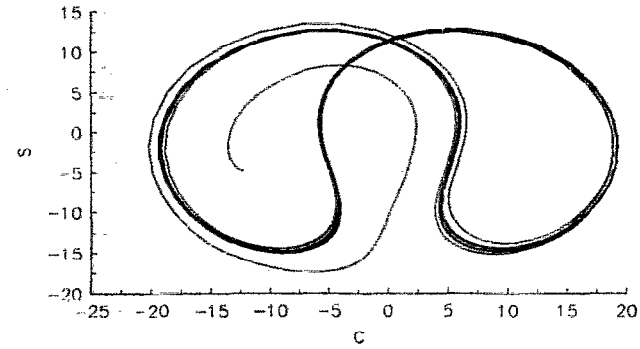

FIG. 9. Stabilization of an otherwise nonstable periodic orbit embedded in the chaotic attractor for $\mathrm{Ra} = 50$, $K_s = 5$, and $P = 4$.

experiments with the Henon map and by Ditto *et al.*[19] in their experiments with a vibrating, magnetostrictive ribbon.

VII. CONCLUSIONS

In this paper, we demonstrated theoretically that active control can be used to significantly alter the flow characteristics of a simple convective system and allow one to obtain desired flow structures. Among other things, the incorporation of the controller allows us to modify the route to chaos, which may ultimately provide us with a new experimental and mathematical means of investigating chaotic attractors.

While we have been able to duplicate some of the ideas presented here in the laboratory[2,20] using a rather crude experimental apparatus, more rigorous verification of the theory awaits the construction of a more refined experimental apparatus. The control techniques we employed here are not necessarily optimal. Better results from a control point of view possibly could be obtained with more sophisticated controllers. However, our major objective was to demonstrate that convection can be controlled by suppressing or enhancing naturally occurring disturbances in the flow. Arguably, the system we have studied is an extremely simple one. The challenge is to examine whether the ideas presented here or similar ones can be implemented in more complicated situations, such as those involving Bénard convection. That is still an open question; but certainly, given the immense potential for applications, it is one that is worth pursuing.

ACKNOWLEDGMENT

This work was supported, in part, by the National Science Foundation through Grant No. CBT 83-51658.

[1] We use the term "laminar" flow to describe flows whose characteristics are predictable in detail.
[2] J. Singer, Y.-Z. Wang, and H. H. Bau, Phys. Rev. Lett. **66**, 1123 (1991).
[3] H. F. Creveling, J. F. De Paz, J. Y. Baladi, and R. J. Schoenhals, J. Fluid Mech. **67**, 65 (1991).
[4] M. Gorman, P. J. Widmann, and K. A. Robins, Phys. Rev. Lett. **52**, 2241 (1984); Physica D **19**, 255 (1986); P. J. Widmann, M. Gorman, and K. A. Robins, Physica D **36**, 157 (1989).
[5] E. Ott, C. Grebogi, and J. A. Yorke, Phys. Rev. Lett. **64**, 1196 (1990). *Soviet–American Perspectives on Nonlinear Science*, edited by D. K. Campbell (AIP, New York, 1990), pp. 153–172.
[6] A. Metrol and R. Greif, in *Natural Convection: Fundamentals and Applications*, edited by W. Aung, S. Kakac, and R. Viskanta (Hemisphere, New York, 1985).
[7] H. H. Bau and K. E. Torrance, Int. J. Heat Mass Transfer **24**, 597 (1981).
[8] J. Singer, MS thesis, University of Pennsylvania, Philadelphia, 1991.
[9] P. Ehrhard and U. Muller, J. Fluid Mech. **217**, 487 (1990). See also Ref. 4.
[10] J. E. Hart, Int. J. Heat Mass Transfer **27**, 125 (1984); **28**, 939 (1985).
[11] A. Yorke, E. D. Yorke, and J. Mallet-Paret, Physica D **24**, 279 (1987).
[12] E. N. Lorenz, J. Atmos. Sci. **20**, 130 (1963).
[13] W. V. R Malkus, Mem. Soc. R. Sci. Liege **IV**, 125 (1972); J. A. Yorke and E. D. Yorke, in *Hydrodynamic Instabilities and the Transition to Turbulence*, edited by H. L. Swinney and J. P. Gollub (Springer-Verlag, Berlin, 1981), pp. 77–96.
[14] C. Sparrow, *The Lorenz Equations: Bifurcations, Chaos, and Strange Attractors* (Springer-Verlag, Berlin, 1982); H. H. Bau and Y.-Z. Wang, *Annual Reviews in Heat* Transfer, edited by C. L. Tien (Hemisphere, New York, 1991), Vol. IV, pp. 1–50.
[15] T. L. Vincent and J. Yu, in *Lecture Notes in Control and Information Sciences*, edited by J. M. Skowronski, H. Flashner, and R. S. Guttalu (Springer-Verlag, Berlin, 1991), pp. 451–465.
[16] Y. Wang, Ph.D. thesis, University of Pennsylvania, 1991.
[17] P. Welander, J. Fluid Mech. **29**, 17 (1967).
[18] D. Auerbach, P. Cvitanovic, J.-P. Eckmann, G. Guanaratne, and I. Procaccia, Phys. Rev. Lett. **58**, 2387 (1987).
[19] W. L. Ditto, S. N. Rauseo, and M. L. Spano, Phys. Rev. Lett. **65**, 3211 (1991).
[20] J. Singer, Y.-Z. Wang, and H. H. Bau, in *Fundamentals of Natural Convection*, edited by T. S. Chen and T. Y. Chu (ASME, New York, 1991).